Cation- and Peptide-Binding Properties of Human Calmodulin-like Skin Protein†

Isabelle Durussel,‡ Bruno Méhul,§ Dominique Bernard,§ Rainer Schmidt,§ and Jos A. Cox*,‡

Department of Biochemistry, University of Geneva, 1211 Genève, Switzerland, and Life Sciences Research, L'Oréal, Centre Charles Zviak, 92583 Clichy, France

Received December 18, 2001; Revised Manuscript Received February 28, 2002

ABSTRACT: Human CLSP, a new Ca^{2+}-binding protein specifically expressed in differentiated keratinocytes, is a 15.9 kDa, four EF-hand containing protein with 52% sequence identity to calmodulin (CaM). The protein binds four Ca^{2+} ions at two pairs of sites with $[Ca^{2+}]_{0.5}$ values of 1.2 and 150 μM, respectively. Mg^{2+} at millimolar concentrations strongly decreases the affinity for Ca^{2+} of the two high-affinity sites, but has no effect on the low-affinity sites. The protein can also bind two Mg^{2+} ($[Mg^{2+}]_{0.5} = 57$ μM) at the sites of high Ca^{2+} affinity. Thus, as fast skeletal muscle troponin C (TnC), CLSP possesses two high-affinity $Ca^{2+}-Mg^{2+}$ mixed sites and two low-affinity Ca^{2+}-specific sites. Studies on the isolated recombinant N- (N-CLSP) and C-terminal half domains of CLSP (C-CLSP) revealed that, in contrast to the case of TNC, the high-affinity $Ca^{2+}-Mg^{2+}$ mixed sites reside in the N-terminal half. The binding of cations modifies the intrinsic fluorescence of the two Tyr residues. Upon Ca^{2+} binding, hydrophobicity is exposed at the protein surface that can be monitored with a fluorescent probe. The Ca^{2+}-dependency of the two conformational changes is biphasic in the absence of Mg^{2+}, but monophasic in the presence of 2 mM Mg^{2+}, both corresponding closely to direct binding of Ca^{2+} to CLSP. In the presence of Ca^{2+}, human CLSP forms a high-affinity 1:1 complex with melittin, a natural peptide considered to be a model for the interaction of CaM with its targets. In the complex, CLSP binds Ca^{2+} with high affinity to all four binding sites. Isolated N- and C-CLSP show only a weak interaction with melittin, which is enhanced when both halves are simultaneously presented to the model peptide.

The major function of the epidermis is the formation of a competent barrier to protect the organism from the external environment and from internal water loss. This task is mainly fulfilled by keratinocytes which proliferate in the basal layer of the epidermis and differentiate into corneocytes during their migration, thus forming the stratum corneum at the surface of the skin. The keratinocyte differentiation program is, in vivo and in vitro, tightly controlled by a Ca^{2+} gradient. In cell cultures in vitro, an extracellular Ca^{2+} concentration between 0.05 and 0.1 mM favors proliferation, whereas $[Ca^{2+}]$ above 1.0 mM induces keratinocyte differentiation (*1*). Two sets of data confirmed the importance of the Ca^{2+} gradient in the control of epidermal differentiation: first, the existence of an in vivo Ca^{2+} gradient was demonstrated in the epidermis (*2*, *3*); and second, changes in the Ca^{2+} gradient following an epidermal barrier disruption were interpreted as a repair signal for keratinocytes, stimulating their proliferation (*4*).

Little information is available concerning the proteins that could mediate these Ca^{2+} signals in the epidermis. During their differentiation process, keratinocytes start to express specific proteins including Ca^{2+}-binding proteins such as profilaggrin (*5*), trichohyalin (*6*), several S100 proteins (*7*), and the CLSP[1] (*8*), a calmodulin-like protein expressed only at very late stages of keratinocyte differentiation just underneath the stratum corneum. CLSP is a very good candidate to participate in the regulation of the final transition of the living keratinocyte to a dead corneocyte, in particular since it was reported to bind transglutaminase 3 (*8*), an enzyme implicated in the formation of the cornified envelope, a key structure of the stratum corneum formed by covalent links between keratins and many other proteins (*9*).

CLSP may be unique in its function in terminal differentiating keratinocytes, yet it belongs to a huge family of Ca^{2+}-binding proteins composed of four EF-hand motifs and devoted to decoding the Ca^{2+} signal in all kinds of cells and tissues. More specifically, CLSP belongs to a small subgroup that strongly resembles CaM, the prototype Ca^{2+}-binding protein closest to the ancestor of the whole family (*10*). To this restricted group belong (in vertebrates) the following: first, CaM-like protein which functions as a light chain of nonconventional myosin X (*11*); second, TnC that regulates contraction in striated muscle; third, the B subunit of calcineurin (CnB) that confers Ca^{2+} regulation to this phosphatase (*12*); and fourth, centrin that is active in centrosome movements and duplication (*13*). Myosin light chains also are close to this family, although they have lost most or all of their capacity to bind Ca^{2+}. For some of these proteins, the three-dimensional structure has been elucidated.

† This work was supported by Swiss National Science Foundation Grant 31-53710.98.

* Corresponding author. E-mail: jos.cox@biochem.unige.ch. Fax: (41)-22-7026483.

‡ University of Geneva.

§ Life Sciences Research, L'Oréal.

[1] Abbreviations: CLSP, calmodulin-like skin protein; N-CLSP, M1−K75 N-terminal half of CLSP; C-CLSP, T71−E146 C-terminal half of CLSP; CaM, calmodulin; TnC, troponin C; TnI, troponin I; ME, melittin, TCA, trichloroacetic acid; TNS, 2-*p*-toluidinylnaphthalene-6-sulfonate; PAGE, polyacrylamide gel electrophoresis.

10.1021/bi016062z CCC: $22.00
Published on Web 04/03/2002

CaM, TnC, and CnB consist of two independent folding units of equal size. In the Ca^{2+} form, these units are in the 'open' conformation with a patch of 800 Å^2 hydrophobic surface exposed to the solvent. In the Ca^{2+}-free form, a 'closed' conformation prevails with the hydrophobic residues buried in the interior of the core in each half. In CaM, the two units are linked by a long α-helix that is prone to unwinding in the middle (*14*). This allows contact and thus cross-talk between the two halves (*15*, *16*). The very close members TnC and CaM display surprisingly different properties: TnC possesses two high-affinity $Ca^{2+}-Mg^{2+}$ mixed sites and two low-affinity Ca^{2+}-specific sites; CaM displays only four low-affinity Ca^{2+}-specific sites.

Many of the target proteins of CaM possess a short amphiphilic α-helical segment, the CaM-binding site, that, when excised from the enzyme, interacts with CaM with characteristics that strongly resemble those in the intact enzyme (*17*). The three-dimensional structure of the CaM−peptide complex reveals that CaM's central helix is kinked and its hydrophobic patches are fully enclosing the α-helix of the target peptide (*18*). Variants of this conformation are also observed for CnB in the holoenzyme and for myosin light chains in myosin. Thus, in this subgroup of Ca^{2+}-binding proteins, a single synergistic unit is formed between the two halves of the protein and the target peptide. A very similar complex is formed between CaM and melittin (ME) (*19*), a bee venom peptide that is considered to be a model for CaM−target protein interaction (*20*).

Here we investigated the cation-binding properties of CLSP and the ensuing conformational changes and found that, with its high- and low-affinity Ca^{2+}-binding sites and a pronounced effect of Mg^{2+}, CLSP is more similar to TnC than to CaM. However, the high-affinity $Ca^{2+}-Mg^{2+}$ mixed sites are located in the N-terminal half of CLSP, contrary to the case of TnC. We also report that CLSP forms a Ca^{2+}-dependent 1:1 and high-affinity complex with ME and both lobes of CLSP contribute to the strength of interaction with ME.

MATERIALS AND METHODS

Materials. Recombinant CLSP and C-CLSP were expressed and purified as described before (*8*). The cDNA coding for truncated CLSP (C-CLSP71−146) was obtained by RT-PCR amplification in pGgex-2T plasmid (clone 46046e7) using *turbo*-pfu polymerase and primer oligonucleotides 5′-gataggatccacggcggcaaggaggcc-3′ and 5′-ttgaattctcactcctgggcgagc-3′ under the following conditions: 1 cycle for 2 min at 95 °C, 30 cycles (94 °C for 1 min, 47 °C for 1 min, 72 °C for 1 min), and 1 cycle at 72 °C for 7 min. The PCR product was gel-purified and digested by *Eco*RI and *Bam*HI restriction enzymes, and then cloned in pGgex-2T as reported before (*8*). Plasmid containing the cloned cDNA was used to transform *E. coli* strain BL21. Expression and purification of C-CLSP were performed according to (*8*) with modifications; the induction of expression was performed using 0.2 mM IPTG at 37 °C for 3−4 h.

For the purification of wild-type N-CLSP, plantar stratum corneum of healthy donors (300 g) was hydrated for 2 days and homogenized at 4 °C in 1800 mL of TBS (25 mM Tris-HCl, pH 7, 500 mM NaCl, 1 mM $MgCl_2$, 2 mM $CaCl_2$, 0.02% sodium azide) containing protease inhibitory cocktail (Complete EDTA-free from Roche Molecular used according to the manufacturer's instructions, complemented with 1 μM pepstatin). The suspension was first filtered on a 40 μm mesh Nylon filter (Millipore). The resulting supernatants were successively passed over 1 and 0.2 μm Polycap filters before chromatographic separation. N-CLSP and intact CLSP were purified on a phenyl-Sepharose column in the presence of 2 mM calcium and eluted from the column by 5 mM EDTA, as described previously (*8*). N-CLSP was separated from undegraded CLSP by gel filtration on a G75HR16/60 column, previously equilibrated in 50 mM phosphate buffer containing 150 mM NaCl at 4 °C. Fractions were analyzed by SDS−PAGE on 15% polyacrylamide gels. The exact sequence of the two halves was determined by amino acid composition, Edman degradation, and mass spectrometry. N-CLSP spans residues 1−75 and C-CLSP 71−146. Melittin was purchased from Sigma and further purified as previously described (*21*).

Metal Ion Removal and Protein Concentration. The protein samples were dialyzed extensively against 50 mM Tris-HCl, pH 7.5, 150 mM KCl (buffer A) containing 1 mM EGTA and put on a 0.8 × 40 cm Sephadex G-25 column equilibrated in buffer A. Occasionally we used the TCA method (*22*). The protein concentration was measured spectrophotometrically using molar extinction coefficients at 276 nm of 3400 M^{-1} cm^{-1} for CLSP and 1700 M^{-1} cm^{-1} for N- and C-CLSP. The extinction coefficient of CLSP was determined by dry weight and is 12% higher than that estimated from the Tyr content as described by Pace et al. (*23*).

Ca^{2+} and Mg^{2+} Binding. Ca^{2+} binding was measured at 25 °C by the flow dialysis method (*24*) in buffer A. Protein concentrations were 20−30 μM. Treatment of the raw data and evaluation of the intrinsic metal-binding constants were as described (*25*). The data were analyzed with the equation of Adair for four binding sites:

$$\nu = \{K_1[Ca^{2+}] + 2K_1K_2[Ca^{2+}]^2 + 3K_1K_2K_3[Ca^{2+}]^3 + 4K_1K_2K_3K_4[Ca^{2+}]^4\}/\{1 + K_1[Ca^{2+}] + K_1K_2[Ca^{2+}]^2 + K_1K_2K_3[Ca^{2+}]^3 + K_1K_2K_3K_4[Ca^{2+}]^4\} \quad (1)$$

where K_1, K_2, etc. are the stoichiometric association constants for the binding of the first and second Ca^{2+} to the protein. The intrinsic association constants, used in this study to present the data, are linked to stoichiometric ones by the statistical factors 4, 3/2, 2/3, and 1/4 (*25*). Mg^{2+}-binding studies were carried out by equilibrium gel filtration at room temperature as reviewed previously (*25*) in buffer A containing 50 μM EGTA, to complex contaminating Ca^{2+}. For Ca^{2+} binding to CLSP in the presence of a 2-fold excess of ME, the buffer used for the perfusion was complemented with 1 μM ME. The antagonism between Ca^{2+} and Mg^{2+} was tested with the competition equation for each site:

$$K'_{Ca}/K'_{Ca,app} = 1 + K'_{Mg,comp}[Mg^{2+}] \quad (2)$$

where K'_{Ca} and $K'_{Ca,app}$ are the intrinsic Ca^{2+}-binding constants for a given site in the absence and presence of Mg^{2+} and $K'_{Mg,comp}$ the calculated Mg^{2+}-binding constant for this site.

Near-UV Difference Spectra. Difference spectra were measured with a Perkin-Elmer λ16 spectrophotometer at room temperature. The protein concentrations were 150 μM for CLSP and 300 μM for N- and C-CLSP. The difference spectra were normalized to molar absorption differences.

Conformational Changes Monitored by Tyr Fluorescence. Emission fluorescence spectra were taken with a Perkin-Elmer LS-5B spectrofluorometer on the metal-free forms of CLSP (20 μM), of N- or C-CLSP (45 μM) in buffer A at 25 °C with excitation at 278 nm and both slits at 5 nm; 20 μM EGTA, or 2 mM Mg^{2+} or Ca^{2+}, or 4 M guanidine hydrochloride was added to monitor the effect of the respective ions or to obtain the spectrum of the denatured protein. The Ca^{2+} dependence of the Tyr fluorescence change was titrated on metal-free protein in buffer A with or without 2 mM Mg^{2+}. The fluorescence intensity was averaged from 302 to 306 nm. The free [Ca^{2+}] was calculated with the speciation program Eqcal of Biosoft (1996) using the Ca^{2+}-binding constants for CLSP reported in this study.

Interaction of CLSP with the Hydrophobic Probe TNS. Changes in the fluorescence properties of 2-*p*-toluidinylnaphthalene-6-sulfonate (TNS) were monitored by fluorometry. After incubation of 2 μM apo protein in buffer A containing either 20 μM EGTA, 2 mM Ca^{2+}, or 2 mM Mg^{2+} with 40 μM TNS for 5 min, the solutions were excited at 328 nm and the emission spectra recorded at 25 °C with 5 nm slits. The Ca^{2+} titrations were carried out on 2 μM metal-free protein in buffer A in the absence or presence of 2 mM Mg^{2+}. Due to contaminating Ca^{2+} in the TNS solution, EDTA up to 5 μM was added. Free [Ca^{2+}] was calculated with the Eqcal program using the Ca^{2+}-binding constants of EDTA (*26*).

Interaction with Melittin. The interaction of CLSP with ME was monitored by Trp fluorometry on an equimolar mixture of 2 μM metal-free CLSP and ME in buffer A. Excitation was at 278 nm; both slits were at 10 nm. EGTA, Ca^{2+}, or Mg^{2+} was added to final concentrations of 50 μM, 1 mM, or 2 mM, respectively, to obtain the respective metal-free, Ca^{2+} and Mg^{2+} forms. The stoichiometry of the CLSP−ME complex could be evaluated from the fluorescence titration in buffer A plus 1 mM Ca^{2+} either of 1.2 μM ME with CLSP increments or of 1.27 μM CLSP with melittin increments (data not shown). Blank titrations were performed to make the necessary subtractions. The interaction between N- or C-CLSP and ME was studied at a 5-fold higher protein concentration. The interactions between CLSP or N-CLSP and ME were also monitored by nondenaturating gel electrophoresis on 10% polyacrylamide gels as previously reported (*20*).

RESULTS

Ca^{2+} and Mg^{2+} Binding to Entire CLSP and N- and C-CLSP. The Ca^{2+}-binding isotherms of CLSP in 0, 0.5, and 2 mM Mg^{2+} determined by flow dialysis are presented in Figure 1 and the affinity constants are summarized in Table 1. The absence of Mg^{2+} displays two sites of high affinity ($[Ca^{2+}]_{0.5}$ = 1.2 μM) with strong positive cooperativity (n_H = 1.99) and two sites of low affinity ($[Ca^{2+}]_{0.5}$ = 150 μM) without any cooperativity. 0.5 mM Mg^{2+} strongly decreases the affinity and allostery of the high-affinity sites for Ca^{2+} ($[Ca^{2+}]_{0.5}$ = 14 μM), but does not affect the low-affinity sites.

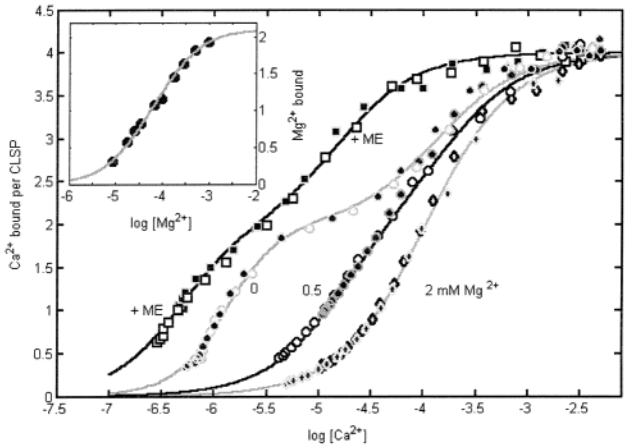

FIGURE 1: Ca^{2+} and Mg^{2+} binding to CLSP at 25 °C in 50 mM Tris-HCl, pH 7.5, 150 mM KCl. Flow dialysis on 25 μM protein in the absence (0) and presence of 0.5 or 2 mM Mg^{2+}. Experiments were carried out in duplicate as shown by marks of different style. Flow dialysis was also carried out in the presence of 1.5 equiv of ME in the absence of Mg^{2+} (squares). All the binding constants are summarized in Table 1. Inset: Mg^{2+} binding performed by equilibrium gel filtration in buffer A containing 50 μM EGTA. The two intrinsic constants amount to 2.3 × 10^4 M^{-1} and 1.1 × 10^4 M^{-1}; n_H equals 0.83, and total binding is 2.1 Mg^{2+} per CLSP.

Table 1: Intrinsic Ca^{2+}-Binding Constants of CLSP[a]

mM Mg^{2+}	K'_1 (M^{-1})	K'_2 (M^{-1})	K'_3 (M^{-1})	K'_4 (M^{-1})
0	7.0 × 10^4	1.4 × 10^6	1.8 × 10^4	1.8 × 10^4
0.5	2.6 × 10^4	3.6 × 10^4	1.4 × 10^4	1.4 × 10^4
	3.4 × 10^3	*7.6 × 10^4*		
2	8.5 × 10^3	8.5 × 10^3	1.1 × 10^4	1.1 × 10^4
	3.6 × 10^3	*8.2 × 10^4*		
ME	6.0 × 10^5	1.3 × 10^6	1.3 × 10^5	1.7 × 10^5

[a] The constants were obtained by iterative fitting of the data of Figure 1 to the Adair equation for four sites. The $K'_{Mg,i,comp}$ values (in italic) were calculated with eq 2. In the experiments with ME, a 1.5-fold excess of peptide was present.

In 2 mM Mg^{2+}, the protein binds four Ca^{2+} with an identical affinity for the four sites ($[Ca^{2+}]_{0.5}$ = 140 μM) and without cooperativity. These data suggest that CLSP possesses two high-affinity sites of the Ca^{2+}−Mg^{2+} mixed type and two low-affinity sites of the Ca^{2+}-specific type. In this respect, CLSP thus shows more resemblance to troponin C (TnC) than to CaM with its four Ca^{2+}-specific sites (*27*). Assuming competition between Ca^{2+} and Mg^{2+} at the two high-affinity sites, the calculated mean $K'_{Mg,comp}$ value [$(K'_{1Mg} \times K'_{2Mg})^{0.5}$, values in italic in Table 1] is 1.7 × 10^4 M^{-1}. Direct Mg^{2+} binding, studied with the equilibrium gel filtration method, shows that 2 ± 0.1 Mg^{2+} ions bind with a mean K'_{Mg} value of 1.6 × 10^4 M^{-1} and an n_H of 0.83 (Figure 1, inset). This is in agreement with the model that the high-affinity sites in CLSP bind Ca^{2+} *and* Mg^{2+}, but Mg^{2+} with a 100-fold lower affinity. In an equilibrium gel filtration experiment in the presence of 500 μM free Ca^{2+} *plus* 500 μM Mg^{2+}, only Ca^{2+} binding was observed. This and conformational data discussed later point to strict competition between Ca^{2+} and Mg^{2+} at the two high-affinity sites and not to the existence of 'auxiliary' Mg^{2+}-binding sites as in the case of calmodulin (*27, 28*).

Studies of the Ca^{2+} affinity and Ca^{2+}−Mg^{2+} selectivity of the isolated N- and C-terminal halves allowed the assignment of the high- and low-affinity sites in CLSP. These

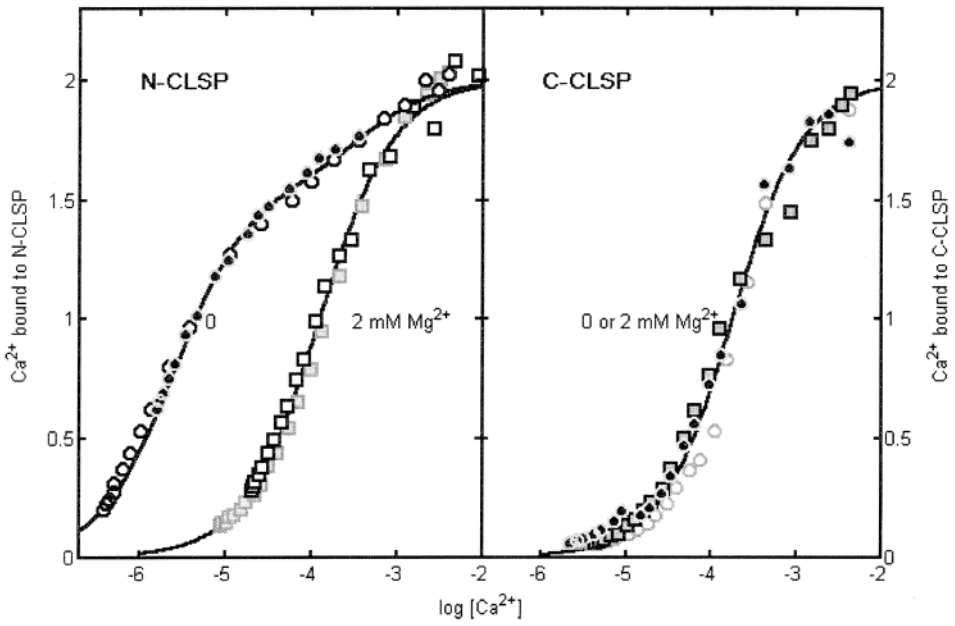

FIGURE 2: Ca^{2+} binding to N- and C-CLSP in conditions described in Figure 1. Flow dialysis on 50 μM protein in the absence (circles) and presence of 2 mM Mg^{2+} (squares). Experiments were carried out in duplicate as shown by marks of different style.

halves contain the intact pairs of N- and C-terminal EF-hands, respectively. Flow dialysis revealed that in the absence of Mg^{2+} Ca^{2+}-binding to N-CLSP is slightly complex with binding of 1.6 Ca^{2+} with a $[Ca^{2+}]_{0.5}$ of 2.5 μM ($n_H = 1.1$), followed by further binding of 0.4 Ca^{2+} with $[Ca^{2+}]_{0.5}$ equal to 200 μM; in the presence of 2 mM Mg^{2+}, N-CLSP binds 2 Ca^{2+} with a $[Ca^{2+}]_{0.5}$ of 125 μM ($n_H = 1.0$) (Figure 2). The calculated $K'_{Mg,comp}$ value is 2.4×10^4 M^{-1}, quite similar to that calculated for the first binding phase in intact CLSP. C-CLSP also binds two Ca^{2+}, but with a $[Ca^{2+}]_{0.5}$ of 170 μM ($n_H = 1.05$), as was observed for the two last binding steps in intact CLSP. 2 mM Mg^{2+} did not noticeably affect the binding of Ca^{2+}. Together these data strongly suggest that the N-terminal domain in intact CLSP contains the high-affinity $Ca^{2+}-Mg^{2+}$ mixed sites whereas the C-terminal domain possesses the two low-affinity Ca^{2+}-specific sites. These data also indicate that the two domains are fairly independent, as was also reported for CaM, TnC, and Ca^{2+}-vector protein, three other members of the subfamily. However, some cross-talk occurs between the two halves since the strong positive cooperativity in the N-domain of the intact protein is lost in the isolated domain and the truncation leads to a loss of high affinity for Ca^{2+} of 20% of the sites.

Secondary Structure by Far-UV Circular Dichroism. The far-UV circular dichroic spectrum of CLSP (data not shown) is very similar to that of most other members of the calmodulin family with an estimated α-helix content of 40−50%. No changes occur upon binding of Ca^{2+} or Mg^{2+}. Although quite unusual for a member of the CaM family (*29*), this was also observed in two centrins (*30*, *31*).

Difference Spectra. Figure 3 shows the UV difference spectra of CLSP (150 μM) induced by addition of 300 μM (to saturate only the high-affinity sites) and 2 mM Ca^{2+} (to saturate all the sites) and of 2 mM Mg^{2+}. The negative twin peaks at 286 and 279 nm are due to Tyr13 and -136, whereas the peaks at 257, 262, and 270 nm are due to Phe. The spectrum is very similar to that of CaM-like protein (*32*), where the twin peak was attributed to Tyr138 (equivalent of Tyr136 in CLSP). Interestingly, 85% of the spectral change occurs upon binding of two Ca^{2+} to the high-affinity sites (light gray versus black line in Figure 3). Mg^{2+} binding leads to much smaller conformational changes. To define the relative contributions of each of the two Tyr residues, the single Tyr13 in the N-terminal domain and the single Tyr136 in the C-terminal domain, we measured the difference spectra of N- and C-CLSP. The normalized Ca^{2+} − apo difference spectrum is 4-fold higher in C-CLSP than in N-CLSP, and the summed difference spectrum is 1.2-fold higher than that of entire CLSP. In contrast, the Mg^{2+} − apo difference spectrum is much more pronounced in N−CLSP than in C−CLSP. The sum of spectra of N- and C-CLSP yields spectra not different from those of entire CLSP. This additivity suggests that there is *no* pronounced cross-talk between the domains in CLSP.

Tyr Fluorescence. Upon excitation of a solution of 20 μM metal-free CLSP at 276 nm, maximal emission fluorescence occurs at 305 nm. Additions of 2 mM Mg^{2+} or Ca^{2+} lead to a 1.3- and 1.9-fold increase, respectively, in fluorescence intensity (Figure 4A). Addition of both Ca^{2+} and Mg^{2+} yields the same spectrum as for Ca^{2+} alone. Denaturation of the protein by addition of 4 M guanidine hydrochloride leads to a 2 nm blue shift of the maximum, but without a change in the intensity of the fluorescence. In N-CLSP, the additions of Mg^{2+} or Ca^{2+} lead to a small change of 1.37- and 1.04-fold, respectively. Upon addition of guanidine hydrochloride, the fluorescence falls to about half, and the latter corresponds to half of that in CLSP. Metal-free C-CLSP shows surprisingly low emission fluorescence, and addition of 4 M guanidine hydrochloride increased the intensity over 6-fold, indicating that the single Tyr136 is strongly quenched in the folded apo protein. Interestingly, the summation spectra of the different forms of N- and C-CLSP spectra are quite similar to those of the corresponding forms of the entire protein, indicating that the rule of additivity is respected. This suggests that the domains are largely independent folding units and confirms our conclusions from direct Ca^{2+} binding and difference spectrophotometry.

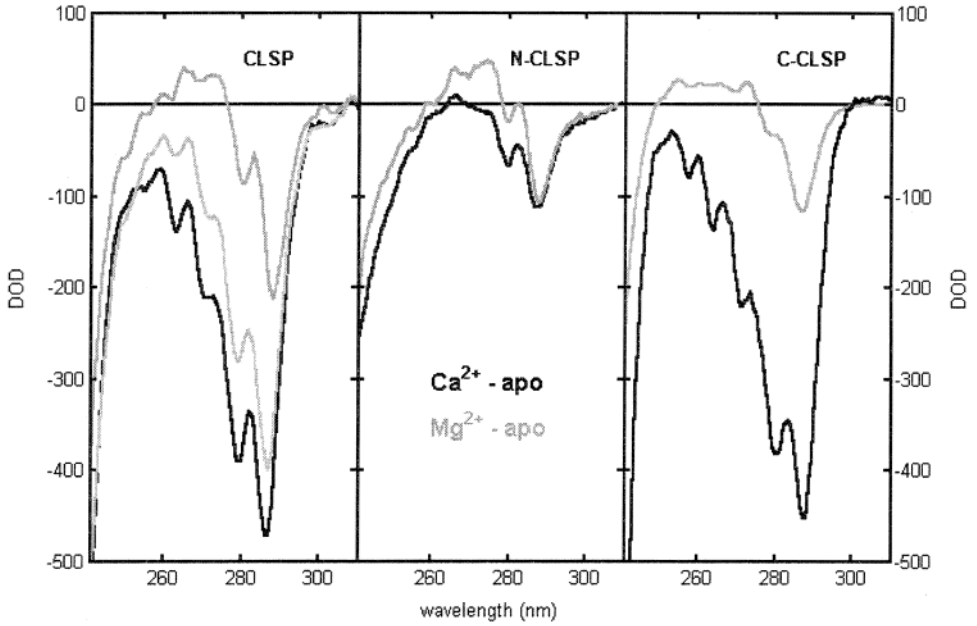

FIGURE 3: Near-UV difference spectra of CLSP, N-CLSP, and C-CLSP. The spectra were taken in buffer A at room temperature and normalized for a protein concentration of 20 μM. 'Ca^{2+} form − apo form' after addition of 2 mM Ca^{2+} (black lines); Mg^{2+} form − apo form after addition of 2 mM Mg^{2+} (dark gray lines). The left panel shows also the difference spectrum after addition of only 2 equiv of Ca^{2+} (light gray line) to CLSP.

The fluorescence titration of 20 μM CLSP with Ca^{2+} in the absence of Mg^{2+} (Figure 4B) shows two phases: the first one with an amplitude of 43% ($[Ca^{2+}]_{0.5}$ = 1.7 μM) and one with an amplitude of 57% ($[Ca^{2+}]_{0.5}$ = 170 μM). The two phases are clearly related to the high- and low-affinity sites, respectively. Strong positive cooperativity in the first phase is observed in both Figure 1 and Figure 4. In the presence of 2 mM Mg^{2+}, the titration with Ca^{2+} shows a single transition with a $[Ca^{2+}]_{0.5}$ of 180 μM and is again reminiscent of the direct Ca^{2+}-binding curve in 2 mM Mg^{2+} (Figure 1, $[Ca^{2+}]_{0.5}$ = 120 μM). Similar titrations on N-CLSP could not be done for lack of a significant Ca^{2+}-dependent signal change. Titration of C-CLSP with Ca^{2+} yielded a single transition with a $[Ca^{2+}]_{0.5}$ of 116 μM and was not affected by Mg^{2+}. These data confirm that the C-terminal half of CLSP harbors the two low-affinity sites and that the binding parameters of this isolated domain are the same as in the whole protein.

TNS Fluorescence Enhancement. A key event in the activation of CaM by Ca^{2+} is the exposure of two hydrophobic patches on its surface, which in turn allows strong interaction with the target enzyme. This event can be monitored with the fluorescence enhancement of the hydrophobic probe TNS (*33*). Ca^{2+}-saturated CLSP enhances the TNS fluorescence 10-fold, but not the apo protein (Figure 5, inset). The spectrum with the Mg^{2+} form is identical to that of the apo form (not shown). The Ca^{2+} titration of this event on a mixture of 2 μM apo CLSP and 40 μM TNS in the absence of Mg^{2+} displays two distinct phases of *equal* amplitude (Figure 5). The first occurs at $[Ca^{2+}]_{0.5}$ = 0.6 μM and n_H = 0.6; the second at 196 μM and an n_H of 1.4. Thus, binding of Ca^{2+} to the pairs of sites in each half, respectively, leads to the exposure of two hydrophobic patches, which are of equal quality as probed with TNS. A similar titration in the presence of 2 mM Mg^{2+} reveals a single conformational transition with $[Ca^{2+}]_{0.5}$ of 120 μM (n_H = 1.4). N- and C-CLSP enhance the fluorescence of TNS to the same extent as CLSP, but at a 2-fold higher molar protein concentration (data not shown). In a Ca^{2+} titration of N-CLSP, a single transition occurs with a half-maximal change at 2 (no Mg^{2+}) or 300 μM Ca^{2+} (2 mM Mg^{2+}). A similar titration on C-CLSP yielded a single transition with a $[Ca^{2+}]_{0.5}$ of 85 μM (n_H of 1.3), corresponding to the low-affinity transition in whole CLSP. These data clearly show that the exposure of the hydrophobic patches in each of the domains is directly governed by the Ca^{2+} affinity of that domain.

Interaction with the Model Peptide Melittin Monitored by Trp Fluorescence. While the interaction of CLSP with TNS reveals the importance of the hydrophobic exposure for the activation of potential targets, a more specific interaction of higher affinity was demonstrated with melittin (ME). ME contains a Trp whose fluorescence strongly increases upon binding of CaM. Figure 6A shows that addition of Ca^{2+} to an equimolar mixture of CLSP and ME leads to a significant (1.3-fold) increase of the fluorescence intensity and a strong blue shift from 352 to 329 nm. In contrast, the apo CLSP *plus* ME spectrum superposes to the calculated sum of the individual components (thin black line), thus strongly suggesting that no complex is formed in the absence of Ca^{2+}. The stoichiometric titration profile of ME with CLSP displays a linear increase and a sharp leveling off at a ratio of 0.99 (not shown), indicative of the formation of a high-affinity (K_D < 20 nM) complex of 1:1 stoichiometry. The spectral changes in the Trp of ME induced by N- and C-CLSP are much more moderate than with entire CLSP and were therefore monitored at 5-fold higher protein and peptide concentrations. Under these conditions, N-CLSP or C-CLSP provokes a 6 or 13 nm blue shift, respectively, of the spectrum of ME (Figure 6B). As a control, no blue shift was observed in the presence of EGTA. Upon increasing the ratio of CLSP halves to ME, a stronger blue shift (N-CLSP) or increase of the fluorescence intensity (C-CLSP) is observed (data not shown), suggesting that each of the

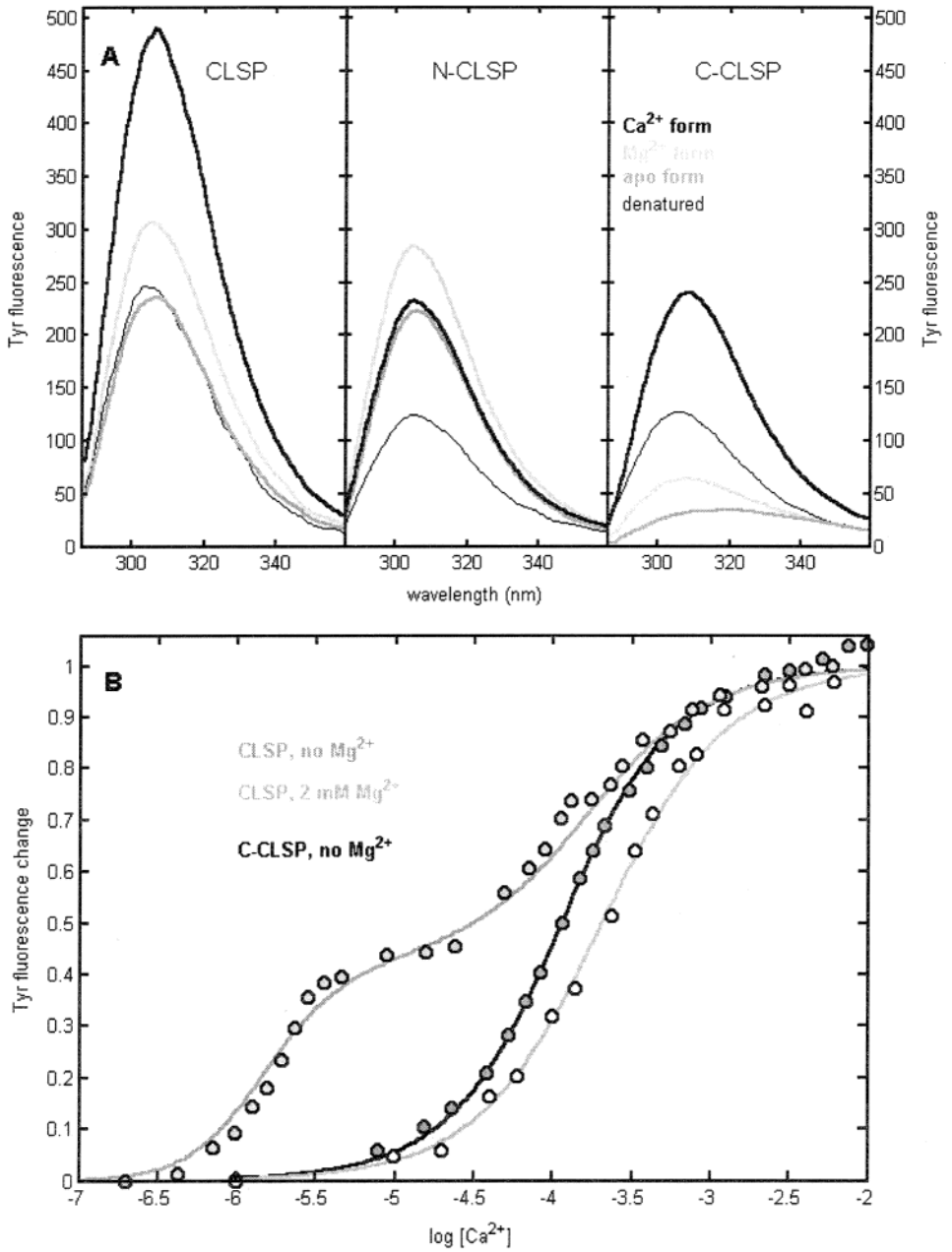

FIGURE 4: (A) Tyr fluorescence spectra of CLSP (20 μM) in buffer A containing 50 μM EGTA (dark gray line), 2 mM Ca^{2+} (thick black line), 2 mM Mg^{2+} (light gray line), or 4 M guanidine hydrochloride (thin black line). Both slits were at 5 nm. To facilitate comparison, the spectra of N- and C-CLSP were also normalized to 20 μM protein concentration. (B) Titration of 20 μM metal-free CLSP by Ca^{2+} in the absence (dark gray line) and presence (light gray line) of 2 mM Mg^{2+}. The biphasic theoretical curve was generated with the following intrinsic binding constants (K'_n): 7.0×10^4, 1.6×10^6, 1.4×10^4, and 1.5×10^4 M^{-1}, and with the following relative contributions: 0, 0.43, 0.285, and 0.285 for the successive binding steps. Black line: titration of 40 μM C-CLSP by Ca^{2+} in the absence of Mg^{2+}. The theoretical curve was generated with the following: $K'_n = 5.5 \times 10^3$ and 1.4×10^4 M^{-1}.

halves can interact with ME, but with a lower affinity than CLSP. Interestingly, the equimolar mixture of N- and C-CLSP (10 μM) yielded the same intensity increase in the spectrum of ME, although not the same blue shift, as intact CLSP (Figure 6B), indicating clearly that the two halves of CLSP can interact simultaneously with the single model peptide, apparently in a cooperative manner.

Direct Ca^{2+} binding to an equimolar mixture of metal-free CLSP and ME revealed a biphasic isotherm in which the affinities of both pairs of sites are increased (Figure 1 and Table 1). Thus, the binding of melittin necessitates that both halves are saturated with Ca^{2+} and acquire their hydrophobic patches. The overall 60-fold increase of Ca^{2+} affinity of all the EF-hand motifs in the complex CLSP·Ca_4·ME seems to be the driving force of the high-affinity interaction of CLSP with ME.

Interaction with Melittin Monitored by Native PAGE. The association of CLSP with ME was confirmed by native PAGE in 10% polyacrylamide gels polymerized in the presence of 3 mM Ca^{2+} (Figure 7A). CLSP migrates with an R_f of 0.56, free ME with its high p*I* does not enter the gel, and the CLSP·Ca_4·ME complex migrates as a single band with an R_f of 0.32. The 1:1 complex is progressively formed when the ratio of ME to CLSP increases. In similar conditions, free CaM migrates with an R_f of 0.62 and CaM·Ca_4·ME with an R_f of 0.57. The complex CLSP·ME was

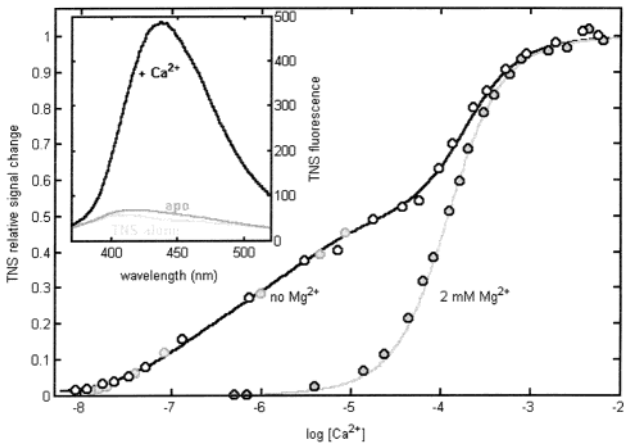

FIGURE 5: TNS fluorescence enhancement by CLSP at 25 °C in 50 mM Tris-HCl, pH 7.5, 150 mM KCl. Titration of the mixture of 2 μM metal-free protein and 40 μM TNS by Ca^{2+} in the absence (black line) and presence (gray line) of 2 mM Mg^{2+}. The signal changes were normalized between 0 and 1. In the absence of Mg^{2+}, the first transition is characterized by $[Ca^{2+}]_{0.5} = 0.6$ μM and $n_H = 0.6$, the second by $[Ca^{2+}]_{0.5} = 196$ μM and $n_H = 1.4$. In the presence of 2 mM Mg^{2+}, $[Ca^{2+}]_{0.5} = 120$ μM and $n_H = 1.4$. Inset: TNS fluorescence spectra in the absence of CLSP (light gray line) and in the presence of CLSP *plus* 2 mM Ca^{2+} (black line), or CLSP *plus* 1 mM EGTA (dark gray line).

not formed if gels were prepared in 1 mM EGTA or in 1 mM EGTA *plus* 2 mM Mg^{2+}, indicating that the apo or Mg^{2+} forms are not able to bind ME (data not shown). When an equimolar mixture of CLSP, CaM, and ME was submitted to PAGE in Ca^{2+}-containing gels, the band corresponding to the CLSP·Ca_4·ME complex was distinctly more intense than the CaM·Ca_4·ME complex (Figure 7B), suggesting that CLSP binds with higher affinity to ME than CaM. Thus, as for CaM (*20*), the dissociation constant of the CLSP·Ca_4·ME complex seems to be in the lower nanomolar range. Native PAGE on a mixture of N-CLSP and increasing molar ratio of ME from 0.2 to 2 lead to the gradual disappearance of the N-CLSP band without the appearance of a distinct new protein band (data not shown). Instead, a gradually more intense smear of protein staining is detected above the N-CLSP band. This confirms that there is interaction between N-CLSP and ME, but of low affinity.

DISCUSSION

CLSP, a new Ca^{2+}-binding protein expressed only in late-stage-differentiating human keratinocytes (*47*), apparently belongs to the restricted CaM family, also called the TNC superfamily (*8*). This family possesses a common genomic pattern (*34*) and comprises the paradigm activator CaM, CaM-like protein, and troponin C, as well as calcineurin B (35% sequence identity to CaM) and centrin (30% identity). CLSP displays 52% sequence identity to CaM; its four EF-hands are fully canonical and in perfect register with those of CaM or fast muscle TnC. Only the central helix is three residues shorter in CLSP than in CaM, but the length of the linker seems not to be very important for the function of CaM (*35*). From this sequence analysis, one can infer that CLSP is closer to CaM, CaM-like protein, and TnC than any other CaBP. Structurally CaM possesses two well-formed separate N- and C-terminal halves that casually interact when the unstable central α-helix unwinds. This interaction becomes strongly synergistic in the presence of a target protein or its representative short target peptide (*17*). Our study shows that in all these aspects CLSP is very similar: the N- and C-terminal halves are independent folding units and show a CaM-like mode of interaction with a model peptide, i.e., simultaneous, cooperative binding of the two domains on a single ME peptide. The three most obvious differences between CaM and TnC are their tissue specificity, selectivity toward targets, and $Ca^{2+}-Mg^{2+}$ selectivity of the cation-binding sites. CaM is ubiquitously expressed in all

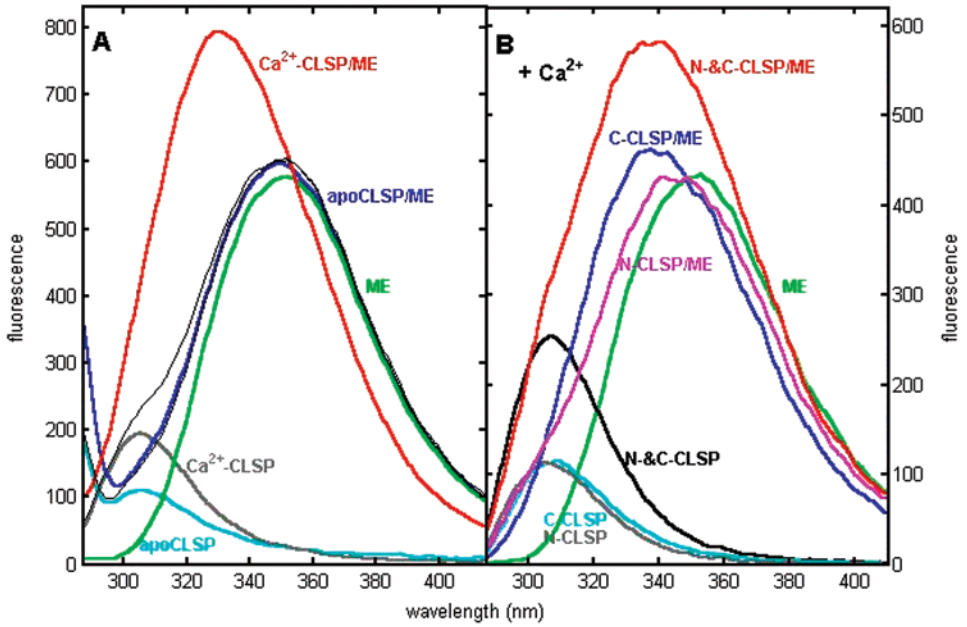

FIGURE 6: (A) Interaction of CLSP with ME measured by Trp fluorescence of ME. 2 μM CLSP and 2 μM ME in buffer A. Ca^{2+}-saturated CLSP + ME (experimental, red line; calculated, black line); metal-free CLSP + ME (experimental, blue line; calculated, black line); ME alone (green line); Ca^{2+}-saturated (gray line); and metal-free CLSP (cyan line). (B) Interaction of N- or C-CLSP or its equimolar mixture with ME. All components were at 10 μM in buffer A. Ca^{2+}-saturated N-CLSP + C-CLSP + ME (red line); Ca^{2+}-saturated N-CLSP (pink line) or C-CLSP (blue line) + ME; ME alone (green line); Ca^{2+}-saturated N-CLSP (gray line); C-CLSP (cyan line) or equimolar mixture (black line).

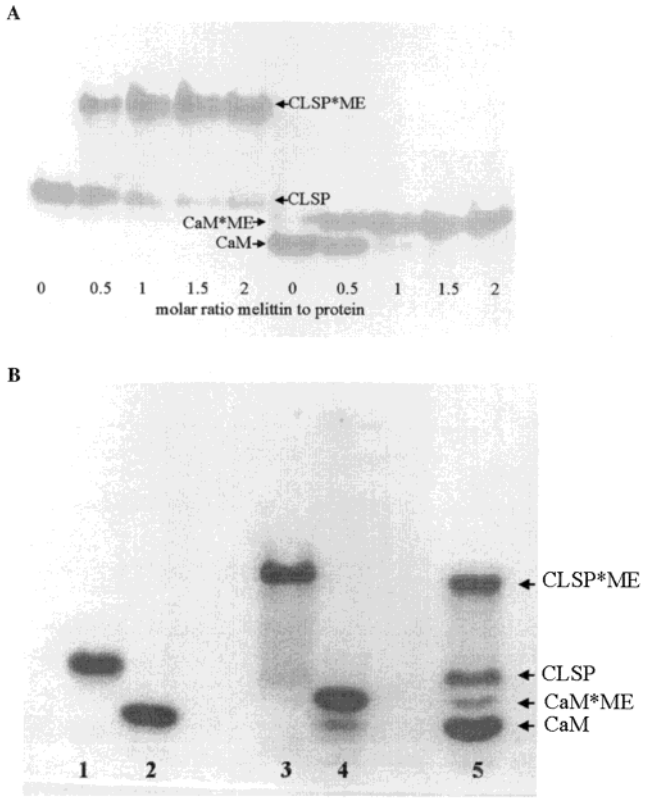

FIGURE 7: Complex formation between CLSP and ME monitored by native PAGE on 10% polyacrylamide gels in the presence of 3 mM Ca^{2+}. Free ME does not migrate in this electrophoretic system. (A) Titration of CLSP (left) or CaM (right) by ME. All samples contained 0.1 nmol of CLSP or CaM and ME in increasing ratios as indicated. (B) Competition of CLSP with CaM for ME. (1) CLSP; (2) CaM; (3) CLSP + 1 equiv of ME; (4) CaM + 1 equiv of ME; (5) equimolar amounts (0.2 nmol) of CLSP + CaM + ME.

types of tissues at protein concentrations from 1 to 10 μM and activates numerous enzymes and cytoskeletal proteins, whereas TnC is only expressed in striated muscle at much higher protein concentrations and interacts only with the other troponin subunits. In this respect, CLSP resembles much more TnC than CaM, since it is exclusively expressed in one tissue. CLSP also may have few target proteins, such as the stratum corneum-specific transglutaminase 3, which interacts with CLSP, but not with CaM.

In its cation-binding properties, CLSP is also more related to TnC than to CaM. CaM binds four Ca^{2+} with nearly equally low affinity centered around 10^5 M^{-1}, and Mg^{2+} moderately antagonizes Ca^{2+} binding to all four sites, not by direct competition, but by binding with low affinity to 'auxiliary' sites (*28*). This cation-binding profile is very different from that of CLSP, which possesses two pairs of sites of very different properties: the pair of high Ca^{2+} affinity (K_{Ca} ca. 10^6 M^{-1}) can also bind strongly Mg^{2+} (K_{Mg} > 10^4 M^{-1}), and this Mg^{2+} competes with Ca^{2+}. The pair of low Ca^{2+} affinity (K_{Ca} = 10^4 M^{-1}) is mostly insensitive to Mg^{2+}. These ion-binding properties resemble those of fast skeletal muscle TnC with its two high-affinity Ca^{2+}−Mg^{2+} mixed sites and two low-affinity Ca^{2+}-specific sites in the C- and N-terminal halves, respectively (*36*). The difference in Ca^{2+} affinity between the high- and low-affinity sites (ca. 20-fold) is similar in CLSP and in TnC.

Besides the similarities, our study revealed two major differences between CLSP and TnC: first, the very strong positive cooperativity in Ca^{2+} binding to the high-affinity sites of CLSP; and second, the location of the high-affinity sites in the N-terminal half of CLSP. The positive cooperativity (n_H = 2) upon binding of Ca^{2+} to the high-affinity sites, which was confirmed in the Tyr fluorescence titration, is specific for Ca^{2+}. Mg^{2+} binding to these same sites displays *negative* cooperativity (n_H = 0.83). This allostery seems to be fragile since it is mostly lost in N-CLSP, the isolated N-terminal half, and also when Mg^{2+} is present. The study of N- and C-CLSP allowed us to determine the precise location of the high- and low-affinity sites. N-CLSP (1−75 segment) binds either two Ca^{2+} or two Mg^{2+}, both with high affinity. Moreover, in N-CLSP, all the conformational changes occur at micromolar Ca^{2+} concentrations in the absence of Mg^{2+}, but they shift to submillimolar $[Ca^{2+}]_{0.5}$ values in the presence of 2 mM Mg^{2+}. Thus, in CLSP the high-affinity sites are located in the N-terminal half, whereas in TnC they are found in the C-terminal half. C-CLSP (71−146 segment) also contains two complete EF-hands and binds specifically two Ca^{2+}, but with low affinity. In TnC, the presence of Ca^{2+} or Mg^{2+} in the C-terminal high-affinity sites is necessary for the anchoring of the subunit to the other troponin subunits (*48*), and Ca^{2+} binding to the N-terminal low-affinity sites triggers contraction (*36*). It is an intriguing, still open question if CLSP also shows such a divergence of functions in its two halves.

The huge discrepancy in the Ca^{2+} affinity of the two pairs of sites allowed us to pinpoint two different conformational events in CLSP. CaM, TnC, and centrins are characterized by a Ca^{2+}-dependent exposure of hydrophobic residues. In CLSP, this pattern is respected for each of its halves: about half of the total TNS fluorescence enhancement occurs upon binding of Ca^{2+} to the high-affinity sites and another half upon binding to the low-affinity sites. Moreover, the isolated N- and C-terminal halves of CLSP enhance the TNS fluorescence to the same extent as the full-length protein, but at a 2-fold higher molar concentration. The profile 'TNS fluorescence enhancement vs $[Ca^{2+}]$' is quite different from the binding isotherm, but this is predicted from the rule of linked functions (*37*, *38*, *44*).

CLSP contains two Tyr residues, one in the N-terminal α-helix of EF-hand I and one in the binding loop of EF-hand IV. In N-CLSP, the fluorescence of Tyr13 is almost insensitive to Ca^{2+} binding, but is sensitive to Mg^{2+} binding. In C-CLSP, the fluorescence of Tyr136 is unusually low in the apo state, likely due to strong quenching since denaturation leads to a strong increase of the fluorescence intensity. But binding of Ca^{2+} also leads to a strong fluorescence increase. In intact CLSP, the microenvironment of both Tyr residues is sensitive to the binding of Ca^{2+}, since the profile 'Tyr fluorescence vs $[Ca^{2+}]$' displays biphasic behavior. Thus, the microenvironments of Tyr13 in the N-domain (43% of total change) and of Tyr136 in the C-domain (57% of total change) are sensitive to cation binding to EF-hands in their own domain, but not to cation binding in the other half. Clear evidence that the N- and C-terminal halves are individual folding units is provided by the effect of Mg^{2+} on these fluorescence changes, since this ion decreases the affinity of only one pair of sites and also shifts the ensuing conformational changes to higher $[Ca^{2+}]_{0.5}$ values. Moreover, Mg^{2+} has a very similar effect on the conformational changes either in N-CLSP or in the N-terminal half of CLSP.

Nevertheless, the two halves show cross-talk, which can be evidenced by probing the very sensitive microenvironments of Tyr and Phe residues. Since most of the changes occur when two Ca^{2+} bind to sites I and II, one would expect that Tyr13 and the two Phe in the N-terminal half are very sensitive to Ca^{2+}. However, in N-CLSP, Tyr13 is 4 times less sensitive than in full-length CLSP, and there is no perturbation in the 250−275 nm range where the Phe microenvironment is probed. It can be deduced that Ca^{2+} binding to the N-terminal sites modifies the microenvironment of Tyr126 and of the three Phe in the C-terminal half. Fluorometry also points to cross-talk: the fluorescence intensity of the single Tyr13 in the apo and Mg^{2+} states of N-CLSP is as high as that of the two Tyr in full-length CLSP, suggesting quenching of Tyr136 in the latter. Cross-talk between the two halves is not so unusual and has been observed in CaM (*39*, *40*) and in CaVP, an invertebrate Ca^{2+}-binding protein with 30% sequence identity to CaM (*41*).

Our study shows that CLSP forms a well-defined, one-to-one, high-affinity and Ca^{2+}-dependent complex with melittin. Of all the Ca^{2+}-binding proteins tested, only CaM, TnC, centrin 2, and CaVP form a complex with similar characteristics. Thus, although this interaction has no physiological significance, the strength and selectivity of the complex clearly define CLSP as a member of the TnC superfamily. Furthermore, our data suggest that the mechanism of activation by CLSP may involve a target-promoted strong increase of the affinity of all the sites for Ca^{2+}. The high affinity of this interaction is quite obvious since, first, the fluorescence titration is stoichiometric and, second, the complex resists the harsh conditions of native PAGE, to which lower affinity complexes (K_d ca. 100 μM) do not resist, such as the one with δ-hemolysin and gramicidin S (*42*, *43*). As in CaM, the high affinity must be due to the synergy between the two halves, which envelope with their own hydrophobic faces the hydrophobic face of the model peptide. With N- and C-CLSP, the shielding of the Trp of ME is much less efficient, but an equimolar mixture of the two CLSP fragments partially mimics the complex formed with the entire CLSP. As reported for CaM (*44*, *45*), we propose for CLSP also a sequential process in which one of the halves binds first to ME; this brings the other half closer so that it can bind ME as well, and this leads to a synergistic increase of the binding affinity.

The considerable differences in the interaction of Ca^{2+} and Mg^{2+} with the respective N- and C-terminal domains of CLSP, which is more or less precisely retained in the halves of the entire protein, suggest a bifunctional role of this protein. In CaM, the binding of Ca^{2+} to the higher affinity C-terminal lobe selectively initiates facilitation of the P/Q (α_{1A}) calcium channel, whereas subsequent Ca^{2+} sensing by the lower affinity N-terminal lobe leads to inactivation of the same channels (*46*). At present, the physiological target of CLSP is not known, but CLSP appears during the terminal differentiation of keratinocytes, where the intracellular free Ca^{2+} levels are supposed to raise gradually from the micromolar to the millimolar range. Thus, the putative physiological function of the N-terminal lobe at micromolar Ca^{2+} levels may well be antagonized when Ca^{2+} binds to the less sensitive EF-hands of the C-terminal lobe. In a much less stringent model, the two lobes of CLSP may regulate two completely different effector proteins. Intrinsically, CLSP possesses the properties for such bifurcation of the Ca^{2+} signal.

ACKNOWLEDGMENT

We thank Dr. Bernard Schwendimann for help with the computer programs.

REFERENCES

1. Hennings, H., Michael, D., Cheng, D., Steinert, P., Holbrook, K., and Yuspa, S. H. (1980) *Cell 19*, 245−254.
2. Menon, G. K., Grayson, S., and Elias, P. M. (1985) *J. Invest. Dermatol. 84*, 508−512.
3. Forslind, B., Lindberg, M., Roomans, G. M., Pallon, J., and Werner-Linde, Y. (1997) *Microsc. Res. Tech. 15*, 373−386.
4. Lee, S. H., Elias, P. M., Proksh, E., Menon, G. K., Mao-Qiang, M., and Feingold, K. R. (1992) *J. Clin. Invest. 89*, 530−538.
5. Markova, N., Marekov, L. N., Chipev, C. C., Gan, S.-Q., Idler, W. W., and Steinert, P. M. (1993) *Mol. Cell. Biol. 13*, 297−182.
6. Lee, S.-C., Kim, I.-G., Marekov, L. N., O'Keefe, E. J., Parry, D. A. D., and Steinert, P. M. (1993) *J. Biol. Chem. 268*, 12164−12176.
7. Heizmann, C. W., and Cox, J. A. (1998) *BioMetals 11*, 383−397.
8. Méhul, B., Bernard, D., Simonetti, L., Bernard, M. A., and Schmidt, R. (2000) *J. Biol. Chem. 275*, 12841−12847.
9. Reichert, U., Michel, S., and Schmidt, R. (1993) in *Molecular biology of the skin* (Darmon, M., and Blumenberg, M., Eds) pp 107−150, Academic Press Inc., London.
10. Nakayama, S., and Krestsinger, R. H. (1994) *Annu. Rev. Biophys. Biomol. Struct. 23*, 473−507.
11. Rogers, M. S., and Strehler, E. E. (2001) *J. Biol. Chem. 276*, 12182−12189.
12. Rusnak, F., and Mertz, P. (2000) *Physiol. Rev. 80*, 1483−1521.
13. Middendorp, S., Küntziger, T., Abraham, Y., Holmes, S., Bordes, N., Paintrand, M., Paoletti, A., and Bornens, M. (2000) *J. Cell Biol. 148*, 405−415.
14. Heidorn, D. B., and Trewhella, J. (1988) *Biochemistry 27*, 909−915.
15. Lee, S. Y., and Klevit, R. E. (2000) *Biochemistry 39*, 4225−4230.
16. Moncrieffe, M. C., Venyaminov, S. Y., Miller, T. E., Guzman, G., Potter, J. D., and Prendergast, F. G. (1999) *Biochemistry 38*, 11973−11983.
17. Chin, D., and Means, A. R. (2000) *Trends Cell Biol. 10*, 322−328.
18. Swindells, M. B., and Ikura, M. (1996) *Nat. Struct. Biol. 3*, 501−504.
19. Kataoka, M., Head, J. F., Seaton, B. A., and Engelman, D. M. (1989) *Proc. Natl. Acad. Sci. U.S.A. 86*, 6944−6948.
20. Comte, M., Maulet, Y., and Cox, J. A. (1983) *Biochem. J. 209*, 269−272.
21. Maulet, Y., and Cox J. A. (1983) *Biochemistry 22*, 5680−5686.
22. Haiech, J., Klee, C. B., and Demaille, J. G. (1981) *Biochemistry 20*, 3890−3897.
23. Pace, C. N., Vajdos, F., Fee, L., Grimsey, G., and Gray, T. (1995) *Protein Sci. 4*, 2411−2423.
24. Colowick, S. P., and Womack, F. C. (1969) *J. Biol. Chem. 244*, 774−777.
25. Cox, J. A. (1996) in *Guidebook to the calcium-binding proteins* (Celio, M. R., Pauls, T., and Schwaller, B., Eds.) pp 1−12, Oxford University Press, Oxford, U.K.
26. Martell, A. E., and Smith, R. M. (1964) in *Critical Stability Constants*, Vol. 1, Plenum Press, New York.
27. Milos, M., Schaer, J.-J., Comte, M., and Cox, J. A. (1986) *Biochemistry 25*, 6279−6297.
28. Milos, M., Comte, M., Schaer, J. J., and Cox, J. A. (1989) *J. Inorg. Biochem. 36*, 11−25.
29. Klee, C. B. (1977) *Biochemistry 16*, 1017−1024.

30. Weber, C., Lee, V. D., Chazin, W. J., and Huang, B. (1994) *J. Biol. Chem. 269*, 15595.
31. Durussel, I., Blouquit, Y., Middendorp, S., Craescu, C. T., and Cox, J. A. (2000) *FEBS Lett. 472*, 208−212.
32. Durussel, I., Rhyner, J. A., Strehler, E. E., and Cox, J. A. (1993) *Biochemistry 32*, 6089−6094.
33. Tanaka, T., and Hidaka, H. (1980) *J. Biol. Chem. 255*, 11078−11080.
34. Yuasa, H. J., and Takagi, T. (2000) *Gene 245*, 275−281.
35. Persechini, A., Blumenthal, D. K., Jarrett, H. W., Klee, C. B., Hardy, D. O., and Kretsinger, R. H. (1989) *J. Biol. Chem. 264*, 8052−8058.
36. Potter, J. D., and Gergely, J. (1975) *J. Biol. Chem. 252*, 2452−2454.
37. Mirzoeva, S., Weigland, S., Lukas, T. J., Shuvalova, L., Anderson, W. F., and Waterson, D. M. (1999) *Biochemistry 38*, 3936−3947.
38. Persechini, A., Yano, K., and Stemmer, P. M. (2000) *J. Biol. Chem. 275*, 4199−4204.
39. Sorensen, B. R., and Shea, M. A. (1998) *Biochemistry 37*, 4244−4253.
40. Protasevich, I., Ranjbar, B., Lobachov, V., Makarov, A., Gilli, R., Briand, C., Lafitte, D., and Haiech, J. (1997) *Biochemistry 36*, 2017−2024.
41. Baladi, S., Tsvetkov, P. O., Petrova, T. V., Takagi, T., Sakamoto, H., Lobachov, V. M., Makarov, A. A., and Cox, J. A. (2001) *Protein Sci. 10*, 771−778.
42. Cox, J. A., Comte, M., Fitton, J. E., and DeGrado, W. F. (1985) *J. Biol. Chem. 260*, 2527−2534.
43. Cox, J. A., Milos, M., and Comte, M. (1987) *Biochem. J. 246*, 495−502.
44. Bayley, P. M., Findlay, W. A., and Martin, S. R. (1996) *Protein Sci. 5*, 1215−1228.
45. Sun, H., and Squier, T. C. (2000) *J. Biol. Chem. 275*, 1731−1738.
46. DeMaria, C. D., Soong, T. W., Aseikhan, B. A., Alvaniam R. S., and Yue, D. T. (2001) *Nature 411*, 484−489.
47. Méhul, B., Bernard, D., and Schmidt, R. (2001) *J. Invest. Dermatol. 116*, 905−909.
48. Cox, J. A., Comte, M., and Stein, E. A. (1981) *Biochem. J.* 195, 205−211.

BI016062Z